Design and Full-Wave Analysis of Cavity-Backed Resistively Loaded Circular-End Bow-Tie Antennas for GPR Applications – Part I

Diego Caratelli and Alexander Yarovoy

Delft University of Technology, IRCTR
Mekelweg 4 – 2628 CD Delft, the Netherlands
d.caratelli@tudelft.nl

Abstract – In this paper, the design of cavity-backed bow-tie antennas for ground-penetrating radars is presented. Dielectric embedding and resistive loading of the radiating structure are employed to achieve at least $30:1$ relative bandwidth ($55\ MHz -> 1.5\ GHz$), with a maximum antenna size of $40\ cm$ and stable antenna performance over different types of the ground. The design procedure is described in detail and provides useful guidelines for the considered class of radiators. Antenna parameters are optimized numerically to combine a large operational bandwidth with reasonably high antenna efficiency. To this end, a full-wave locally conformal finite-difference time domain procedure useful to model electromagnetic structures having complex geometrical and electrical characteristics in the vicinity of the ground is adopted.

Index Terms – Bow-tie antenna, dielectric embedding, ground-penetrating radar, locally conformal finite-difference time-domain modeling, resistive loading.

I. INTRODUCTION

Antennas for ground-penetrating radars (GPR) must meet severe specifications regarding low-frequency operation, broadband characteristics, small volume occupation, and reasonable efficiency for good signal-to-noise ratio of the radar image [1]. Due to increase with frequency of the radio wave attenuation in geophysical media, typical GPR operates at the frequencies below $1\ GHz$. The operational frequency range is determined by the particular application and its relation to the nature of the target, soil constitution, desired depth of penetration, and inversion/classification method being used. For example, a desirable frequency range for detecting subsurface utilities (like water and gas pipes, cables, etc.) is thought to be from $100\ MHz$ to $1\ GHz$ [1]. While low frequencies within this frequency range can be used for subsurface utilities detection via near-field coupling, high frequencies can be used for accurate ranging. For either impulse or stepped-frequency continuous-wave ($SFCW$) radio transmission technique, the adoption of broadband antennas with relative bandwidth above 100% is essential. But, the broadband characteristics must not be obtained at the expense of either the efficiency or the antenna volume. Furthermore, it is required that GPR antennas exhibit stable performance over different types of ground keeping the same wavelet and magnitude of the radiated field. In addition, high isolation between transmit and receive antennas is required to reduce the parasitic mutual coupling. In short, large operational bandwidth at low frequencies, ground invariant performance, high efficiency, small size, and good isolation in an antenna pair, which are sometimes mutually conflicting requirements, are all to be satisfied [2].

As known, cavity-backed spiral and bow-tie antennas might be a suitable choice in GPR applications [3–5]. The spiral antennas possess a large fractional bandwidth. However, their dispersion nature results in an extended time response of the radiated electromagnetic field, and consequently either hardware or software decon-

volution of the received radio signal is needed. As spiral antenna performance depends on properties of the ground, such deconvolution often fails to provide good results [1]. Furthermore, reflections from the ends of the arms cause both clutters and degradation of the circularity of the polarization, while the proximity of the ground adversely affects the reactive field of the antenna, resulting in a significant degradation of its characteristics in terms of radiation pattern, and input impedance. The bow-tie antennas, which basically are the limiting case of biconical antennas, are attractive mainly due to their construction simplicity and wideband property [3–4], and they are widely employed in *GPR* applications [1], [8– 13]. Bow ties with circular ends and some resistive loading demonstrate reduced late-time ringing [5–7]. Cavity-backing is used to decrease the back-radiation level in the air region [13]. However, the operational bandwidth of cavity-backed bow ties exceeds rarely $30\% - 40\%$, which is considerably below the desired figure of merit (100%).

In this paper, we have designed a novel *GPR* antenna featuring an extremely large fractional bandwidth (more than 100%), good transient behavior, ground invariant performance, reasonably high bandwidth, electrically small size, low mutual coupling in an antenna pair, and low back radiation. The antenna is designed to be used with *SFCW* radar and targeted antenna specifications are: the operational frequency band, based on the reflection coefficient with respect to $50\ \Omega$ feeding line, from $100\ MHz$ to $1\ GHz$ $(10:1$ relative bandwidth); maximal antenna size of $40\ cm$ by $40\ cm$ by $30\ cm$ (length $\times$ width $\times$ height); coupling between Tx and Rx antennas in the radar system below $-30\ dB$. Neither in literature nor in commercial systems, antennas with similar specifications have been found. For the antenna optimization and performance analysis a dedicated locally conformal finite-difference time-domain ($FDTD$) procedure, useful to accurately analyze electromagnetic structures having complex geometrical and electrical characteristics and to take into account the impact of the ground, is adopted. The design procedure is described thoroughly and provides useful guidelines for the considered class of radiators. Detailed analysis of circuital and radiation properties of the antenna is presented in Part II of this paper.

This paper is organized as follows. The proposed antenna structure is briefly described in Section II. The full-wave *FDTD*-based modeling approach for the electromagnetic characterization of the proposed antenna is discussed in Section III. Finally, Section IV describes the optimization and design guidelines of the antenna.

II. THE PROPOSED ANTENNA STRUCTURE AND DESIGN

The proposed antenna is based on a circular-ended bow tie (see Fig. 1). The initial radiator consists of two circularly-ended flairs, whose electrical conductivity σ_f varies with the radial distance ρ from the feeding delta gap. Dielectric embedding and resistive loading of the radiating structure are used to reduce the flair angle while keeping antenna input impedance at $50\ \Omega$ and compacting the antenna size [5]. To reduce parasitic emission to air, the antenna is cavity-backed. Special cavity filling is suggested in order to keep wideband antenna matching. The loading profile is optimized based on numerical simulations.

To design such an antenna we use the following procedure:

1. determine the dielectric embedding;
2. determine the bow-tie flair angle based on the required antenna impedance;
3. determine the optimal resistive loading.

The first two steps are based on analytic techniques while the last one requires numerical simulations.

A. The absorber-filled cavity

To reduce the antenna back-radiation level, potentially resulting in *EMI*s with nearby electronic equipment, a suitable shielding structure is adopted (see Fig. 1). This in turn is useful to meet the severe restrictions of the allowed

transmitted power level usually imposed by local authorities.

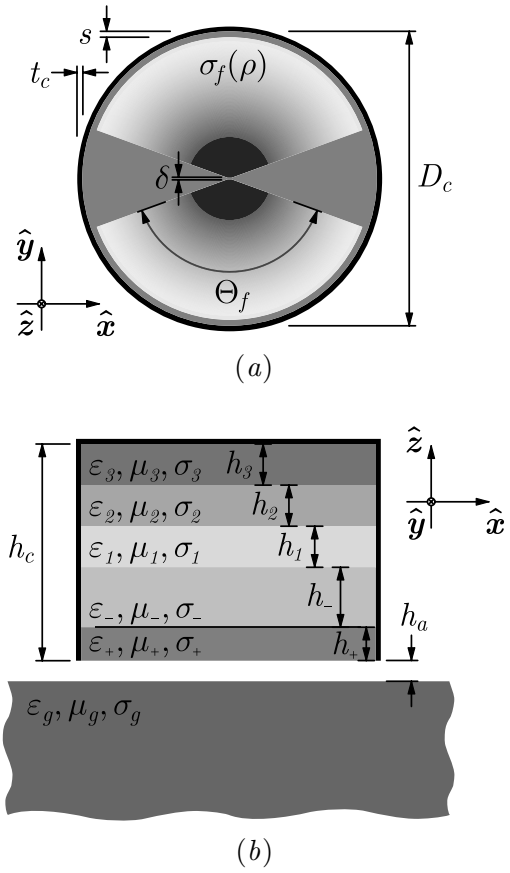

Fig. 1. Bottom (a) and cross-sectional (b) view of the cavity-backed resistively-loaded bow-tie antenna for *GPR* applications. Antenna characteristics: $D_c = 40\ cm$, $s = 1\ cm$, $t_c = 0.5\ cm$, $\Theta_f = 130°$, $\delta = 0.25\ cm$, $h_c = 28.5\ cm$, $h_a = 3\ cm$, $\varepsilon_{r_g} = 6$, $\sigma_g = 0.015\ S/m$, $h_+ = 0.5\ cm$, $\varepsilon_{r_+} = 3$, $\sigma_+ = 0\ S/m$, $h_- = 10\ cm$, $\varepsilon_{r_-} = 10$, $\sigma_- = 0\ S/m$, $h_1 = 6\ cm$, $\varepsilon_{r_1} = 11$, $\sigma_1 = 0.125\ S/m$, $h_2 = 6\ cm$, $\varepsilon_{r_2} = 15$, $\sigma_2 = 0.25\ S/m$, $h_3 = 6\ cm$, $\varepsilon_{r_3} = 20$, $\sigma_3 = 1\ S/m$. The reference system adopted to express the field quantities is shown.

The considered cavity may be regarded as an inhomogeneously filled circular waveguide, terminated on a perfectly conducting wall, where the spatial distribution of the electromagnetic field can be represented as the superposition of an infinite number of modes. The voltage and current relevant to each mode can be conveniently evaluated using the transmission-line formalism [14]. The description of the electromagnetic field within the structure is thereby reduced to the description of the electrical behavior of an infinite set of transmission lines terminated on an ideal short circuit (see Fig. 2). The input impedance of each transmission line can be easily evaluated as

$$Z_- = Z_{c-} \frac{Z_1 \cos k_- h_- + j Z_{c-} \sin k_- h_-}{Z_{c-} \cos k_- h_- + j Z_1 \sin k_- h_-}, \quad (1)$$

where

$$Z_i = Z_{c_i} \frac{Z_{i+1} \cos k_i h_i + j Z_{c_i} \sin k_i h_i}{Z_{c_i} \cos k_i h_i + j Z_{i+1} \sin k_i h_i}, \quad (2)$$

for $i = 1, 2, 3$, and $Z_4 = 0$. In (1) and (2) k_-, Z_{c-} and k_i, Z_{c_i} denote the propagation constant and characteristic impedance of the generic mode within the antenna substrate and the $i-$th absorbing layer ($i = 1, 2, 3$), respectively. The thickness and electrical properties of such materials have been determined by imposing, at the central working frequency $f_c = 550\ MHz$, the

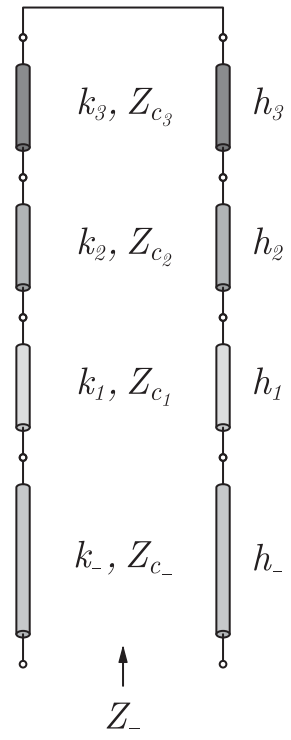

Fig. 2. Transmission-line equivalent circuit of the generic electromagnetic mode propagating in the antenna cavity.

matching condition

$$|\Gamma_-| < 0.05\,, \tag{3}$$

being

$$\Gamma_- = \frac{Z_- - Z_{c-}}{Z_- - Z_{c-}} \tag{4}$$

the input reflection coefficient relevant to the transmission-line equivalent circuit relevant to the fundamental mode (TE_{11}) propagating within the cavity. In (3) the manufacturing constraint $\varepsilon_{r-} \leq 10$ has been also enforced. By doing so, the parameters specified in the caption of Fig. 1 have been obtained. In particular, by selecting the relative permittivity of the superstrate as $\varepsilon_{r-} = 10$ we set the cut-off frequency of the fundamental mode of the cavity to be equal to about $139\ MHz$. Below such frequency, the cavity essentially behaves like a reactive load for the antenna. It should be pointed out that the absorbing panels to be embedded in the shielding cavity can be realized using suitable filled polymer composites [15–16]. The electrical properties of such materials can be conveniently adjusted by properly setting the volume fraction of the ceramic and ferrite filler.

Finally, the permittivity of the antenna substrate has been selected to be $\varepsilon_{r+} = 3$ in order to achieve a smooth transition from the antenna feeding line to homogeneous soils with relative dielectric constant $\varepsilon_{r_g} \geq 3$, so minimizing the return-loss level in the operating frequency band.

B. The bow-tie flair angle

A resistively-loaded bow-tie antenna may be regarded as a coplanar fin transmission line, whose characteristic impedance, according to quasi-static theory [17], can be calculated using the relevant static capacitance. A model to evaluate such capacitance by conformal mapping is proposed in [18]. As a result, the above-mentioned characteristic impedance is expressed as follows

$$Z_0 = \frac{\eta_0}{\sqrt{\bar{\varepsilon}_r}} \frac{K(k)}{K(k')}\,, \tag{5}$$

where $K(\cdot)$ is the complete elliptic integral of the first kind [19] with moduli

$$k = \frac{1 - \sin\Theta_f/2}{1 + \sin\Theta_f/2}\,, \tag{6}$$

$$k' = \sqrt{1 - k^2}\,, \tag{7}$$

η_0 denotes the free-space characteristic impedance, and $\bar{\varepsilon}_r = \left(\varepsilon_{r+} + \varepsilon_{r-}\right)/2$ is the effective relative permittivity value at the dielectric interface (see Fig. 1), where the antenna flairs are realized. Consequently, by imposing the impedance matching condition $Z_0 = R_g$, the flairs angle Θ_f can be easily determined. So, in order to achieve the input impedance of $50\ \Omega$, we have to select the antenna flair angle of 150°.

III. THE FULL-WAVE ANTENNA MODELING

The analysis and design of complex radiating structures requires accurate electromagnetic field prediction models. One such widely used technique is the finite-difference time-domain ($FDTD$) algorithm. However, in the conventional formulation proposed by Yee [20–21], each cell in the computational grid is implicitly supposed to be filled by a homogeneous material. For this reason, the adoption of Cartesian meshes could result in reduced numerical accuracy when structures having curved boundaries are to be modeled. In this case, the locally conformal $FDTD$ scheme in [22–23] provides clear advantages over the use of the stair-casing approach or unstructured and stretched space lattices, potentially suffering from significant numerical dispersion and/or instability. Such a scheme, necessary to improve the numerical accuracy of the conventional algorithm, is based on the definition of effective material parameters suitable to describe the geometrical and electrical characteristics of complex electromagnetic structures [22]. By using the mentioned subcell method, the design and accurate full-wave analysis of the considered class of ultra-wideband bow-tie antennas have been carried out.

As shown in Fig. 1, the radiating structure is assumed to be elevated to a height $h_a = 3\ cm$ over the ground, modeled as a lossy homogeneous half-space having relative permittivity $\varepsilon_{r_g} = 6$ and electrical conductivity $\sigma_g = 0.015\ S/m$, corresponding to the asphalt. A voltage source of amplitude $V_g = 1\ V$ and in-

ternal resistance $R_g = 50\ \Omega$ is employed to excite the structure. The locally conformal *FDTD* characterization of the structure has been performed by making use of a non-uniform computational grid with maximum cell size $\Delta h_{\max} = \lambda_{\min}/16 \simeq 0.5\ cm$, where $\lambda_{\min}$ is the operating wavelength inside the ground at the maximum frequency $f_{\max} = 1.5\ GHz$ in the excitation signal, which is a Gaussian pulse of the form

$$\mathcal{P}(t) = \exp\left[-\left(\frac{t-t_0}{\tau_g}\right)^2\right], \qquad (8)$$

where $t_0 = 10\tau_g$, and

$$\tau_g = \frac{\sqrt{\ln 10}}{\pi f_{\max}}. \qquad (9)$$

The selection of τ_g according to (9) gives the source pulse significant energy in the frequency band up to $f_{\max}$. The pulse is coupled into the finite-difference equations used to update the electric field distribution within the feeding delta gap. As usual, the antenna input voltage $V_{in}(t)$ and current $I_{in}(t)$ are related to the normalized incident and reflected waves by

$$a(t) = \frac{1}{2}\left[\frac{V_{in}(t)}{\sqrt{Z_0}} + I_{in}(t)\sqrt{Z_0}\right], \qquad (10)$$

$$b(t) = \frac{1}{2}\left[\frac{V_{in}(t)}{\sqrt{Z_0}} - I_{in}(t)\sqrt{Z_0}\right]. \qquad (11)$$

Therefore, the antenna input reflection coefficient can be easily determined as

$$\Gamma_{in}(f) = \frac{\mathsf{F}[b(t)]}{\mathsf{F}[a(t)]}, \qquad (12)$$

where $\mathsf{F}[\cdot]$ denotes the Fourier transform operator.

In all calculations presented in this paper, a ten-cell uniaxial perfectly matched layer (*UPML*) absorbing boundary condition for lossy media [24] has been used at the outer *FDTD* mesh boundary to simulate the extension of the space lattice to infinity. As outlined in [21], the *UPML* is indeed perfectly matched to the inhomogeneous medium formed by the upper air region and the lossy material half space modeling the ground. So, no spurious numerical reflections take place at the air-ground interface. In particular, a quartic polynomial grading of the *UPML* conductivity profile has been selected in order to have a nominal reflection error $R_{PML} \simeq e^{-16}$.

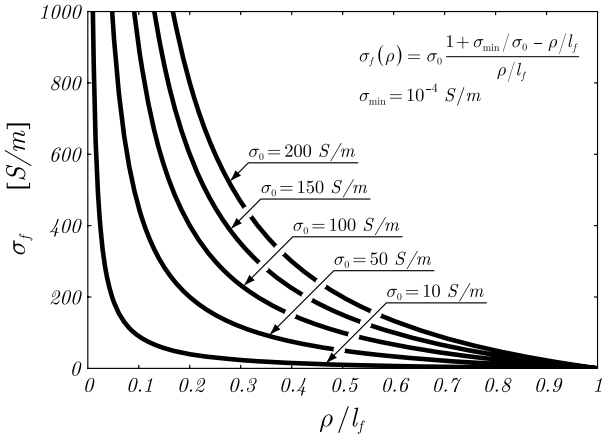

Fig. 3. Resistive loading profile of the cavity-backed circular-end bow-tie antenna flairs.

For the individual antenna elevated above ground, the total *FDTD* mesh dimensions are $282 \times 283 \times 253$ in the x, y, z directions respectively, and the computational time is approximately $1.4\ s$ per step on a workstation provided with a $2.33\ GHz$ Intel Xeon processor.

IV. THE ANTENNA OPTIMIZATION

It is commonly understood that in *GPR* applications for detection of buried objects, it is essential that the probing pulse exhibits reduced late-time *ringing* in order to prevent masking of the targets. Late-time *ringing* is caused mainly by the multiple reflections between the antenna open ends and the feed point, which are responsible for the narrowband behavior of the radiating structure. To properly enlarge the antenna bandwidth (thus reducing the late-time *ringing*), we apply to the flairs of the proposed radiator a resistive loading with distribution

$$\sigma_f(\rho) = \sigma_0 \frac{1 + \sigma_{\min}/\sigma_0 - \rho/l_f}{\rho/l_f}, \qquad (13)$$

similar to the ideal *Wu-King* profile (see Fig. 3). In (13), $l_f = D_c/2 - s_c = 19\ cm$ is the flair

length, which is determined from the maximal allowed size of the antenna, and $\sigma_{\min} = \sigma_f(l_f)$ is the electrical conductivity value at the antenna end sections. In particular, the considered resistive loading can be easily realized by means of well-established technologies extensively used in printed circuit board (PCB) manufacturing and lithographic processes, such as thick film printing on ceramic, etched printed circuit technology, and screen printed ink technology [25]. Among these, screen printed ink technology appears to be the most robust and flexible. In fact, inks can be mixed to any required resistance within bounds, and the profile can be built up from many layers, thus eliminating the possibility of inter-segment discontinuities.

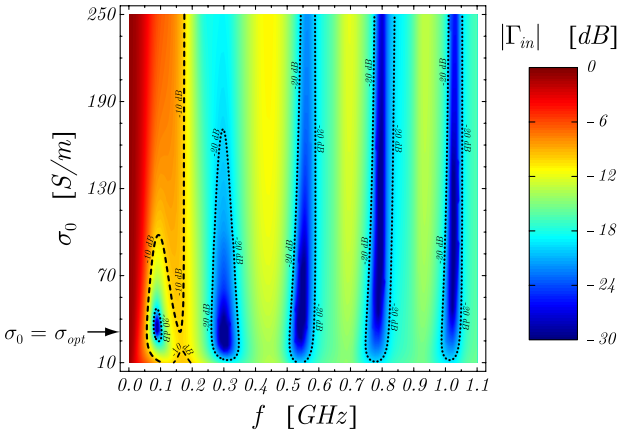

Fig. 4. Frequency behavior of the antenna input reflection coefficient for different loading profiles. The antenna is elevated $3\ cm$ over the ground, modeled as a lossy homogeneous half-space having relative permittivity $\varepsilon_{r_g} = 6$ and electrical conductivity $\sigma_g = 0.015\ S/m$.

A specific parametric analysis has been carried out to determine an optimal value of the parameter σ_0 appearing in (13) which results in achieving the lowest operational frequency, the operational bandwidth above $1\ GHz$, and a reasonably high efficiency (see Fig. 4). The total antenna efficiency is given by

$$e_a(f) = e_r(f)\, e_{in}(f)\ , \tag{14}$$

where

$$e_r(f) = \frac{P_{rad}(f)}{P_{in}(f)}\ , \tag{15}$$

$$e_{in}(f) = 1 - |\Gamma_{in}(f)|^2 \tag{16}$$

are the radiation and input mismatch efficiency terms, respectively. In (15), $P_{in}(f) = \frac{1}{2}\mathrm{Re}\{V_{in}(f)\, I_{in}^*(f)\}$ is the real input power accepted by the antenna, while the total radiated power $P_{rad}(f)$ can be determined by integrating the real part of the Poynting vector over a surface S_a in the air region, enclosing the radiating structure, namely

$$P_{rad}(f) = \frac{1}{2}\mathrm{Re}\left\{\iint_{S_a} \underline{E}(\underline{r}, f) \times \underline{H}^*(\underline{r}, f) \cdot \underline{dS}\right\}. \tag{17}$$

It has been numerically found that the value $\sigma_0 = \sigma_{opt} \simeq 30\ S/m$ provides a good compromise between impedance matching and efficiency. In particular, with the specified resistive loading profile, the antenna exhibits an extremely large operational bandwidth (based on the reflection coefficient) from $55\ MHz$ to at least $1.5\ GHz$. Inspection of Fig. 5 also reveals that $e_a(f)$ assumes reasonably high values ($> 15\%$) in the low-frequency band, but rapidly decreases at higher frequencies because of the

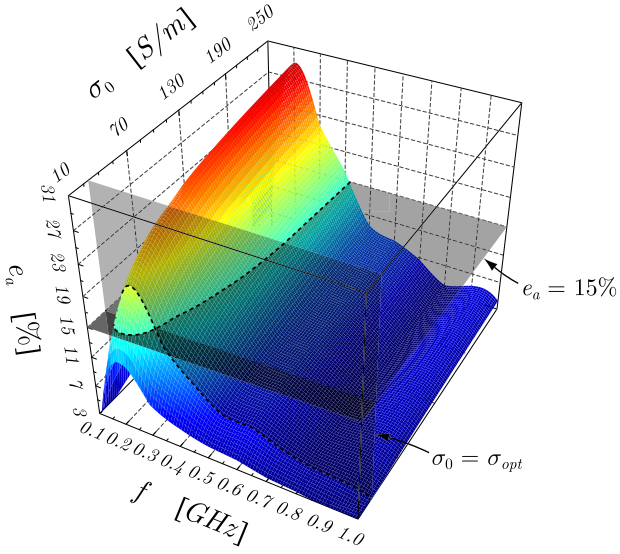

Fig. 5. Frequency behavior of the antenna efficiency for different loading profiles. The antenna is elevated $3\ cm$ over the ground, modeled as a lossy homogeneous half-space having relative permittivity $\varepsilon_{r_g} = 6$ and electrical conductivity $\sigma_g = 0.015\ S/m$.

loading effect of the cavity, and the proximity effect of the ground. In particular, by increasing the conductivity parameter σ_0, the total efficiency becomes larger, since the material forming the antenna flairs tends to behave like a perfect electric conductor, so leading to an overall reduction of the ohmic losses level. Unfortunately, a significant low-frequency degradation of the antenna return-loss occurs for $\sigma_0 \gtrsim \sigma_{opt}$, or $\sigma_0 \lesssim \frac{3}{4}\sigma_{opt}$. From a physical point of view, this means that the radio waves due to the field reflection from the antenna ends, as well as from the air-ground interface and the metallic cavity walls, contain significant energy when returning to the feed point. It's worth noting that a non-flat frequency behavior of the antenna radiation efficiency can be responsible for a spreading of the electromagnetic pulse transmitted by the radiator. However, since the proposed structure is mainly intended for *SFCW* radar applications, a suitable power equalization technique can be conveniently adopted to guarantee a uniform level of radiated energy [26].

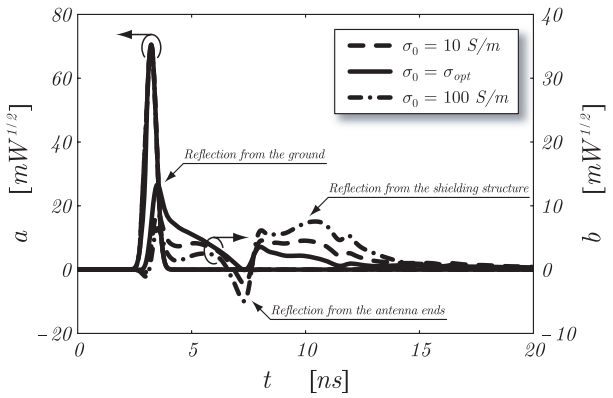

Fig. 6. Time-domain behavior of the normalized incident and reflected waves at the antenna input terminals for different loading profiles. The antenna is elevated $3\,cm$ over the ground, modeled as a lossy homogeneous half-space having relative permittivity $\varepsilon_{r_g} = 6$ and electrical conductivity $\sigma_g = 0.015\ S/m$.

Figure 6 clearly illustrates some key effects of the resistive loading distribution along the antenna flairs. Shown is the time-domain behavior of the normalized waves $a(t)$, $b(t)$ at the input terminals of the radiator. In particular, the peak at $\sim 3.2\ ns$ represents the incident voltage pulse. Those at $\sim 3.5\ ns$, $\sim 7.2\ ns$, and $\sim 10\ ns$ correspond, respectively, to reflections from the ground, the antenna ends, and the shielding structure, which should be minimal for a well-designed *GPR* system. As it appears, highly conducting loading profiles ($\sigma_0 > \sigma_{opt}$) reduce the reflections from the ground, whereas increasing the resistivity ($\sigma_0 < \frac{3}{4}\sigma_{opt}$) is an effective means to lower reflections from the edges of the antenna panels and the shielding structure. So, the optimal loading distribution ($\sigma_0 = \sigma_{opt}$) represents a trade-off between the above-mentioned operation modes.

V. CONCLUSION

We have designed a cavity-backed loaded bow-tie antenna for ground-penetrating radars. Dielectric embedding and resistive loading of the radiating structure are used to reduce the flair angle and the antenna size, as well as to assure stable antenna performance over different types of the ground. In order to reduce parasitic emission to air, the antenna is cavity-backed. Special cavity filling is suggested in order to keep wideband antenna matching. The antenna exhibits an extremely large operational bandwidth (based on the reflection coefficient) from $55\ MHz$ to at least $1.5\,GHz$, radiation efficiency level comparable with Wu-King dipoles, electrically small size of $40\ cm$ by $40\ cm$ by $29\ cm$ (length × width × height). Furthermore (as it is shown in Part II), the antenna has ground invariant performance and mutual coupling below $-30\ dB$ in a pair configuration.

The antenna optimization and circuital performance investigation have been carried out numerically by means of a dedicated full-wave technique based on a locally conformal *FDTD* scheme, which does not require the stair-case approximation and, thus, ultimatively suits for accurate modeling of structures with cylindrical shape. From the numerical optimization, it has been found that the conductivity value $\sigma_{opt} \simeq 30\ S/m$ results in an optimal resistive loading distribution in terms of the lowest operating frequency, the largest absolute operational

bandwidth and reasonable efficiency. For this loading profile, the antenna with maximum size of about $40\ cm$ is matched to the $50\ \Omega$ feeding line starting from the frequency $f_\ell \simeq 55\ MHz$.

At the lowest operational frequency, the normalized volume featured by the antenna is given by $V/\lambda_0^3 \simeq 0.025\%$, being λ_0 the relevant free-space wavelength. Thus, the proposed antenna exhibits a strongly reduced volume occupation. Despite that, it has been numerically demonstrated that the antenna efficiency assumes reasonably high values ($> 15\%$) in the low-frequency band, while it decreases at higher frequencies because of the loading effect of the cavity and the proximity effect of the ground. It should be noticed that the efficiency of a dipole of similar dimensions with the ideal *Wu-King* loading profile in free space is below 15%. Thus, the efficiency of the proposed antenna is comparable with that of an ideal *Wu-King* dipole antenna.

Finally, it has been shown that starting from $f \simeq 200\ MHz$ variations of the loading profile do not cause considerable differences in the antenna efficiency which means that the efficiency is not much affected by the resistive loading of the radiating flairs.

ACKNOWLEDGMENT

This research has been carried out in the framework of *EU*-sponsored project *ORFEUS* (contract number: *FP6-2005-Global-4-036856*). The authors would like to thank anonymous reviewers for their suggestions and comments.

REFERENCES

[1] D. Daniels, *Ground Penetrating Radar*, 2^{nd} ed., IEE Press, 2004.

[2] A. G. Yarovoy and L. P. Ligthart, "Theoretical and experimental analysis of GPR antennas," in *Proc. URSI EMTS International Symposium on Electromagnetic Theory*, Pisa, Italy, vol. 1, pp. 108–110, May 23-27, 2004.

[3] W. L. Stutzman and G. A. Thiele, *Antenna Theory and Design*, 2^{nd} ed., Wiley-Interscience, 1998.

[4] C. A. Balanis, *Antenna Theory: Analysis and Design*, 3^{rd} ed., Wiley-Interscience, 2005.

[5] D. Caratelli, "Design and analysis of antennas for ground penetrating radar applications," Delft University of Technology, the Netherlands, Tech. Rep. IRCTR–S–041–07, Sept. 11, 2007.

[6] D. Caratelli, "Full-wave analysis of cavity-backed resistively loaded bow-tie antennas for GPR applications," Delft University of Technology, the Netherlands, Tech. Rep. IRCTR–S–001–08, Jan. 11, 2008.

[7] D. Caratelli, A. Yarovoy, and L. P. Ligthart, "Full-wave analysis of cavity-backed resistively-loaded bow-tie antennas for GPR applications," *European Microwave Conference 2008*, Amsterdam, the Netherlands, pp. 204-207, October 27-31, 2008.

[8] G. H. Brown and O. M. Woodward Jr., "Experimentally determined radiation characteristics of conical and triangular antennas," *RCA Rev.*, vol. 13, pp. 425–452, Dec. 1952.

[9] K. L. Shlager, G. S. Smith, and J. G. Maloney, "Optimization of bow-tie antennas for pulse radiation," *IEEE Trans. Antennas Propagat.*, vol. 42, pp. 975–982, July 1994.

[10] A. A. Lestari, A. G. Yarovoy, and L. P. Ligthart, "RC-loaded bow-tie antenna for improved pulse radiation," *IEEE Trans. Antennas Propagat.*, vol. 52, pp. 2555–2563, Oct. 2004.

[11] A. A. Lestari, A. G. Yarovoy, and L. P. Ligthart, "Adaptive wire bow-tie antenna for GPR applications," *IEEE Trans. Antennas Propagat.*, vol. 53, pp. 1745–1754, May 2005.

[12] B. Lampe and K. Holliger, "Resistively loaded antennas for ground-penetrating radar: A modeling approach," *Geophysics*, vol. 70, pp. 23–32, May-June 2005.

[13] Y. Nishioka, O. Maeshima, T. Uno, and S. Adachi, "FDTD analysis of resistor-loaded bow-tie antennas covered with ferrite-coated conducting cavity for subsurface radar," *IEEE Trans. Antennas Propagat.*, vol. 47, pp. 970-977, June 1999.

[14] R. E. Collin, *Foundations for Microwave Engineering* , 2^{nd} ed., Wiley-IEEE Press, 2000.

[15] D. R. Saini, V. M. Nadkarni, P. D. Grover, and K. D. P. Nigam, "Dynamic mechanical, electrical and magnetic properties of ferrite filled styrene-isoprene-styrene," *Journal of Materials Science*, vol. 21, pp. 3710-3716, Oct. 1986.

[16] Emerson & Cuming microwave products. Eccostock HiK500F technical datasheet. Avail-

able online at: http://www.eccosorb.com/file/861/ek-025%20eccostock%20hik500f%20.pdf

[17] K. C. Gupta, R. Garg, and I. J. Bahl, *Microstrip Lines and Slotlines*, Artech House, 1979.

[18] R. L. Carrel, "The characteristic impedance of two infinite cones of arbitrary cross section," *IRE Trans. Antennas Propagat.*, vol. 6, pp. 197–201, Apr. 1958.

[19] M. Abramovich and I. A. Stegun, *Handbook of Mathematical Functions*, Dover Publications, 1968.

[20] K. S. Yee, "Numerical solution of initial boundary value problems involving Maxwell's equations," *IEEE Trans. Antennas Propagat.*, vol. 14, pp. 302–307, May 1966.

[21] A. Taflove and S. C. Hagness, *Computational Electrodynamics: The Finite-Difference Time-Domain Method*, 3^{rd} ed., Artech House, 2005.

[22] D. Caratelli and R. Cicchetti, "A full-wave analysis of interdigital capacitors for planar integrated circuits," *IEEE Trans. Magnetics*, vol. 39, pp. 1598–1601, May 2003.

[23] D. Caratelli, R. Cicchetti, G. Bit-Babik, and A. Faraone, "A perturbed E-shaped patch antenna for wideband WLAN applications," *IEEE Trans. Antennas Propagat.*, vol. 54, pp. 1871-1874, June 2006.

[24] S. D. Gedney, "An anisotropic perfectly matched layer-absorbing medium for the truncation of FDTD lattices," *IEEE Trans. Antennas Propagat.*, vol. 44, pp. 1630-1639, Dec. 1996.

[25] DEMINE partners. Public Report D16, European Project 29902 DEMINE, 2002. Available online at: http://www.eudem.vub.ac.be/files/demine_final_ report.pdf

[26] R. Persico and G. Prisco, "A reconfigurative approach for SF-GPR prospecting," *IEEE Trans. Antennas Propagat.*, vol. 56, pp. 2673-2680, Aug. 2008.

Diego Caratelli was born in Latina, Italy on May 2, 1975. He received the Laurea (summa cum laude) and Ph.D. degrees in Electronic Engineering from "La Sapienza" University of Rome, Italy in 2000 and 2004, respectively. In 2005, he joined as a Contract Researcher the Department of Electronic Engineering, "La Sapienza" University of Rome. Since 2007, he is with the International Research Centre for Telecommunications and Radar (*IRCTR*) of Delft University of Technology, the Netherlands, as a Senior Researcher.

His main research activities include the design, analysis and experimental verification of printed microwave and millimeter-wave passive devices and wideband antennas for satellite, *WLAN* and *GPR* applications, the development of analytically based numerical techniques devoted to the modeling of electromagnetic field propagation and diffraction processes, as well as the analysis of *EMC/EMI* problems in sensitive electronic equipment.

Dr. Caratelli was the recipient of the 2010 Young Antenna Engineer Prize at the 32th European Space Agency Antenna Workshop. He is a member of the Italian Electromagnetic Society (*SIEm*).

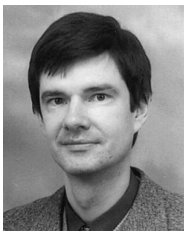

Alexander G. Yarovoy (M'96-SM'04) graduated from the Kharkov State University, Ukraine, in 1984 with the Diploma with honor in radiophysics and electronics. He received the Candidate Phys. & Math. Sci. (Ph.D. equivalent) and Doctor Phys. & Math. Sci. (D.Sc. equivalent) degrees in radiophysics in 1987 and 1994, respectively.

In 1987, he joined the Department of Radiophysics at the Kharkov State University as a Researcher and became a Professor there in 1997. From September 1994 through 1996, he was with Technical University of Ilmenau, Germany as a Visiting Researcher. Since 1999, he is with the International Research Centre for Telecommunications-Transmission and Radar (*IRCTR*) at the Delft University of Technology, the Netherlands. Since 2009, he leads there a chair of Microwave Technology and Systems for Radar. His main research interests are in ultra-wideband (*UWB*) microwave technology and its applications (in particular, *UWB* radars) and applied electromagnetics (in particular, *UWB* antennas).

Prof. Yarovoy is the recipient of a 1996 International Union of Radio Science (*URSI*) "Young Scientists Award" and the European Microwave Week Radar Award in 2001 for the paper that best advances the state-of-the-art in radar technology (together with L.P. Ligthart and P. van Genderen). Prof. Yarovoy served as the Chair of the 5th European Radar Conference (*EuRAD'08*), Amsterdam, The Netherlands, and Co-Chairman and the Technical Program Committee Chair of the Tenth International Conference on Ground Penetrating Radar (*GPR2004*), Delft.